

Article

Cytochrome P450 3A2 and PGP-MDR1-Mediated Pharmacokinetic Interaction of Sinapic Acid with Ibrutinib in Rats: Potential Food/Herb–Drug Interaction

Muzaffar Iqbal ¹, Mohammad Raish ^{2,*}, Ajaz Ahmad ³, Essam A. Ali ¹, Yousef A. Bin Jardan ²,
Mushtaq A. Ansari ⁴, Mudassar Shahid ², Abdul Ahad ², Khalid M. Alkharfy ³ and Fahad I. Al-Jenoobi ²

- ¹ Department of Pharmaceutical Chemistry, College of Pharmacy, King Saud University, Riyadh 11451, Saudi Arabia; muziqbal@ksu.edu.sa (M.I.); esali@ksu.edu.sa (E.A.A.)
- ² Department of Pharmaceutics, College of Pharmacy, King Saud University, Riyadh 11451, Saudi Arabia; ybinjardan@ksu.edu.sa (Y.A.B.J.); mahmad1@ksu.edu.sa (M.S.); aahad@ksu.edu.sa (A.A.); aljenobi@ksu.edu.sa (F.I.A.-J.)
- ³ Department of Clinical Pharmacy, College of Pharmacy, King Saud University, Riyadh 11451, Saudi Arabia; aajaz@ksu.edu.sa (A.A.); alkharfy@ksu.edu.sa (K.M.A.)
- ⁴ Department of Pharmacology and Toxicology, College of Pharmacy, King Saud University, Riyadh 11451, Saudi Arabia; muansari@ksu.edu.sa
- * Correspondence: mraish@ksu.edu.sa



Citation: Iqbal, M.; Raish, M.; Ahmad, A.; Ali, E.A.; Bin Jardan, Y.A.; Ansari, M.A.; Shahid, M.; Ahad, A.; Alkharfy, K.M.; Al-Jenoobi, F.I. Cytochrome P450 3A2 and PGP-MDR1-Mediated Pharmacokinetic Interaction of Sinapic Acid with Ibrutinib in Rats: Potential Food/Herb–Drug Interaction. *Processes* **2022**, *10*, 1066. <https://doi.org/10.3390/pr10061066>

Academic Editors: Malgorzata Starek and Monika Dąbrowska

Received: 28 April 2022

Accepted: 23 May 2022

Published: 26 May 2022

Publisher's Note: MDPI stays neutral with regard to jurisdictional claims in published maps and institutional affiliations.



Copyright: © 2022 by the authors. Licensee MDPI, Basel, Switzerland. This article is an open access article distributed under the terms and conditions of the Creative Commons Attribution (CC BY) license (<https://creativecommons.org/licenses/by/4.0/>).

Abstract: Ibrutinib (IBR) metabolism (primarily by CYP3A enzyme) is the main route of excretion for IBR, which could lead to drug–drug/herb–drug interactions with herbal medicines, nutritional supplements, and other foods. Sinapic acid (SA) is a bioactive phytonutrient that is used as a dietary supplement to treat a variety of illnesses. Pharmacokinetic interactions may occur when IBR interacts with SA, which influences the pharmacokinetic processes such as absorption, distribution, metabolism, and excretion. Therefore, it is obligatory to investigate the safety apprehensions of such parallel usage and to evaluate the possible impact of SA on the pharmacokinetics of IBR and propose a possible interaction mechanism in an animal model. The IBR concentration in plasma samples was determined using a validated UHPLC-MS/MS method after administration of a single oral dosage of IBR (50 mg/kg) in rats with or without SA pretreatment (40 mg/kg p.o. each day for 7 days, $n = 6$). The co-administration of IBR with SA displayed significant increases in $C_{max} \sim 18.77\%$, $AUC_{0-T} \sim 28.07\%$, $MRT \sim 16.87\%$, and $K_{el} \sim 24.76\%$, and a significant decrease in the volume of distribution $V_z/F_{obs} \sim 37.66\%$, the rate of clearance $(Cl/F) \sim 21.81\%$, and $T_{1/2} \sim 20.43\%$, respectively, were observed as compared to rats that were administered IBR alone, which may result in increased bioavailability of IBR. The metabolism of IBR in the liver and intestines is significantly inhibited when SA is given, which may lead to an increase in the absorption rate of IBR. These findings need to be investigated further before they can be used in clinical practice.

Keywords: ibrutinib; sinapic acid; pharmacokinetics; pharmacodynamics; drug interaction

1. Introduction

Chemotherapeutics for various malignancies are increasingly shifting from time-limited, traditional, uncertain cytotoxic chemotherapy cycles to reliable oral treatment with targeted protein-designated treatments. In this line, relapsed/refractory chronic lymphocytic leukaemia (CLL) with 17p deletion has shown excellent results with Burton's tyrosine kinase (BTK), an irreversible inhibitor of a critical signalling protein in the B cell receptor (BCR) pathway [1,2]. Using an irreversible bond with cysteine-481 in the active region of BTK (TH/SH1 domain), the powerful BTK inhibitor ibrutinib (IRB) elicits remarkable responses in B cell malignancies and blocks phosphorylation of BTK at tyrosine 223 with an IC_{50} of 0.5 nM of more than 24 h [3,4]. BTKs are recommended for sustained periods, oftentimes in patients with comorbidities. In this way, they are consistently co-directed

alongside medicines at risk of drug–drug interactions. This angle has been, to some degree, tended until now, calling for extensive examination. IBR is absorbed and metabolized entirely from the gastrointestinal tract (GI) and via the liver and intestines [5]. It is primarily metabolized by cytochrome P450 (CYP) 3A into a dihydrodiol metabolite of IBR that inhibits BTK, with approximately 15-times lower activity than that of IBR [6]. There is low bioavailability of IBR (560): 3.9% under fasting and 8.4% under fed conditions [7]. The extensive first-pass metabolism plays a crucial role, rather than the poor absorption in the GI tract and poor bioavailability of IBR [5,7]. Therefore, the concomitant use of botanical dietary supplements or herbs or drugs (CYP3A inducer or inhibitor) with IBR may change the pharmacokinetics and pharmacodynamics parameters by inhibiting or inducing CYP3A drug-metabolizing enzymes; inhibition or inducers of these enzymes can result in longer or shorter half-lives, higher or lower exposure, and lower or higher clearances of therapeutic agents, and further increase the potential for toxicity or subtherapeutic effects [4–9]. Moreover, IBR treatment is associated with life-threatening toxicities such as thrombocytopenia, atrial fibrillation/flutter, diarrhoea, pneumonia, progressive multifocal leukoencephalopathy, hypertension, and prolongation of the PR interval and hyperuricemia [10] (Janssen Inc. IMBRUVICA® product monograph. Toronto, ON, Canada; 24 July 2018).

SA (3,5-dimethoxy-4-hydroxycinnamic acid) is a polyphenolic acid and a nutraceutical and dietary supplement with good oral bioavailability [11]. It exists in fruits [12], nuts [13], spices, vegetables, cereals [14] of plants belonging to the Brassicaceae family [15,16], and coffee and tea [17]. The widespread use of SA in conventional medication is attributable to its medicinal properties, such as chemopreventive, antioxidant, antihypertensive, anti-inflammatory, antiaging, hepatoprotective, antihyperglycaemic, cardioprotective, antihyperlipidaemic, antimutagenic, antihypertensive, anticancer, neuroprotective, antidepressant, and antibacterial activities, etc. SA is widely used in different foods, such as organic products, flavours, vegetables, oil, and grains. SA is effectively available in food, with a long history of human use, and poses no risk of harm [11,18–20]. In a cross-sectional analysis of the UK National Diet and Nutrition Survey Rolling Programme [21], an estimated daily intake of 46.3 to 78.9 mg/day for children and 153.6 to 231.8 mg/day for adults was determined in HCA derivatives such as SA, ferulic acid, and p-coumaric acid, which are commonly consumed in high doses. However, this intake varies significantly between individuals. Another study found that men and women consume an average of 222 mg of phenolic acids per day, with SA accounting for 200 mg of this total. Vegetables, fruits, nuts, and coffee are the most common dietary sources of HCAs, accounting for 63% of SA and 59% of p-coumaric acid, respectively [22]. SA is in the range of 0.25 and 0.21 g/kg fresh weight [23]. IBR are substrates of CYP3A and dependent on auto-induction [24]. The majority of serious cases of drug interactions occur due to the interference of the metabolic clearance of one drug by another co-administered drug, food, or natural product. Pharmacokinetic interactions may occur when IBR interacts with SA and influences the pharmacokinetic processes such as absorption, distribution, metabolism, and excretion. Therefore, it is obligatory to investigate the safety apprehensions of such parallel usage, as previously reported, which significantly inhibits the CYP3A2-, CYP2C11-, and P-glycoprotein/MDR1-mediated metabolism of carbamazepine in the liver and intestine [25]. The pharmacokinetic interaction of IBR with dietary supplements, resveratrol [26], and naringenin [27] in rats and grapefruit juice [28] in healthy volunteers has been reported in previous studies, which did not use a mechanistic approach. However, the potential pharmacokinetic IBR interactions with SA have still not been investigated; thus, to explore the probable interaction mechanism, the present study was designed.

2. Materials and Methods

2.1. Materials

IBR and SA were purchased from Sigma-Aldrich (St. Louis, MO, USA). Formic acid, acetonitrile, ammonium acetate, and methanol (UHPLC grade) were procured from

BDH, Pool, (Dorset, UK) and the primary antibodies Anti-CYP3 A2 (sc-271033) and anti- β -actin (LS-C147034) antibodies were purchased from Santa Cruz (California, CA, USA).

2.2. Mass Spectrometry and UHPLC Chromatographic Conditions

Quantitative measurement of IBR in rat plasma samples was performed using UHPLC-MS/MS, a combination of ultra-high-performance liquid chromatography and tandem mass spectrometry [29]. Using an Acquity BEH C₁₈ column with a flow rate of 0.3 mL/min, both IBR and the internal standard (dasatinib) were separated and eluted by a mobile phase comprising acetonitrile with 0.1 percent formic acid and 20 mM ammonium acetate in a ratio of 80:20 (*v/v*) with a run time of 2.5 min. In contrast, the auto-temperature sampler was set at 10 °C, while the column oven was kept at 40 °C. To ionise the samples, we employed electrospray ionisation in positive mode. The calibration curves of IBR were linear in plasma samples between the concentration ranges of 2.12 and 1000 ng/mL. IBR and IS were quantified in MRM mode using the parent-to-daughter ion transition of 441.16 > 84.04 for IBR and 488.06 > 401.11 for IS, respectively. The capillary voltage (2.6 kV), source (150 °C), and desolvation (350 °C) temperatures were tuned for the greatest sample ionisation performance. Nitrogen (650 L/h flow) and argon (0.016 mL/minute flow) were employed as the desolvation gas and collision gas, respectively. Moreover, 48 and 46 V cone voltages and 40 and 28 eV impact energies were used for the analyte and IS, respectively. Following the "US Food and Drug Administration 2018 guideline for bioanalytical technique validation", the assay was validated in terms of the precision and accuracy. The allowed variance in precision and accuracy, both within and between days, was found to be 15%. Data was collected with Masslynx software 4.1 SCN 805, and sample processing was performed using TargetLynks.

2.3. Sample Preparation

In a 2 mL Eppendorf tube, 150 μ L plasma sample was transferred and 15 μ L internal standard (2.5 μ g/mL) was spiked and vortex-mixed appropriately. Then, 1 mL of ethyl acetate was added into each tube for liquid-liquid extraction. After vortex-mixing, samples were transferred to a shaker for 15 min followed by cold centrifugation (4 °C) at 11,500 rpm for 10 min. The upper organic layer was transferred to a 1.5 mL capacity Eppendorf tube and transferred to the sample concentrator (maintained at a medium temperature) for drying. The dried residue was reconstituted with 150 μ L acetonitrile and 5 μ L transferred to UPLC-MS/MS for analysis.

2.4. Animals Studies

The research was approved by the Research Ethics Committee of King Saud University College of Pharmacy Riyadh, Saudi Arabia (KSU-SE-21-58). The NIH Guideline for the Care and Use of Laboratory animals was followed for all animals used in the experiments. Before the experiment, the animals were given free access to food and drink, but they were fasted the night before. Male 18-week-old Wistar rats were housed in polyamide rat cages, with a 12-h light/dark cycle, at 25 °C \pm 2 °C in accordance with the regulations for animal facilities for 1 week prior to the study. After a 12-h fast, the rats were divided into four groups of six each. For seven days, rats in group I (the vehicle control) were administered normal saline orally. IBR (50 mg/kg) was administered to the rats in group II after six days of normal saline. One hour after administering SA to the rats in groups III and IV, IBR (50 mg/kg) was administered orally. In heparinized tubes, blood samples were taken from the tail vein at intervals of 0, 0.5, 1, 1.5, 2, 3, 4, 6, 12, and 24 h after the injection of IBR (50 mg/kg). IBR analysis was carried out using UPLC-MS/MS on blood samples centrifuged at 3500 \times g for 10 min to extract plasma, which was then transferred to 1.5 mL tubes for analysis. Afterwards, the rats were decapitated, and liver and intestinal tissue were harvested for Western blotting.

2.5. Pharmacokinetic Analysis

In PK Solver (version 1.0), the pharmacokinetic parameters were calculated using the non-compartmental model. A number of variables were investigated, including the maximum concentration (C_{max}), time to maximum concentration (AUMC), area under the concentration–time curve (AUC), elimination rate constant (K_{el}), half-life ($T_{1/2}$), mean residence time (MRT), volume of distribution (V_z/F), and clearance (CL/F).

2.6. Protein Expression Analysis

Hepatic and intestine total cytosolic protein levels were measured using a Pierce™ BCA Protein Assay Kit (Thermo Fisher Scientific, Waltham, MA USA) [30]. Immunoblotting was carried out as described by [31]. Polyacrylamide gels with 10% SDS were electrophoresed with 25 µg protein, transferred to activated PVDF membranes, and blocked using a blocking solution (4% skim milk and BSA in TBS of 1% Tween 20). Antibodies against intestine, liver, and kidney CYP3A2 isozymes and β -actin were used to incubate the membrane overnight at 4 °C. After washing with 1%, Tween TBS, and TBS, the membrane was incubated for 2 h at room temperature with the appropriate secondary antibodies. Scanning of the bands was accomplished using Luminata™ Western Chemiluminescent Horse Radish Peroxidase Substrates (Millipore, Billerica, MA, USA). The immunoblots were subjected to densitometric evaluation (LI-COR C-Di-Git Blot Scanners) (Lincoln, NE, USA).

2.7. Statistical Analysis

Dunnett's multiple comparison test or one-way analysis of variance (ANOVA) were used to determine the significance of the sample; $p < 0.05$ was considered significant.

3. Results

3.1. Effect of SA on IBR Pharmacokinetics

The pharmacokinetic parameters of IBR are represented in Table 1 and Figure 1. After oral administration of IBR, the C_{max} was 486.60 ± 15.71 ng/mL with a T_{max} of 1 h. For animals that were co-administered SA, C_{max} of 577.95 ± 19.97 ng/mL and T_{max} of 1 h of IBR were found. IBR co-administered with SA displayed significant increases in C_{max} ~18.77%. The $AUC_{(0-T)}$ ~28.07%, MRT ~16.87%, and K_{el} ~24.76%, and a significant decrease in the volume of distribution V_z/F ~37.66%, the rate of clearance CL/F ~21.81%, and $T_{1/2}$ ~20.43%, respectively, compared to rats that were administered IBR alone were observed. This may result in increased bioavailability due to substantial inhibition of CYP3A2- and Pgp/MDR1-mediated IBR metabolism in the liver and intestine, which may increase the IBR absorption rate.

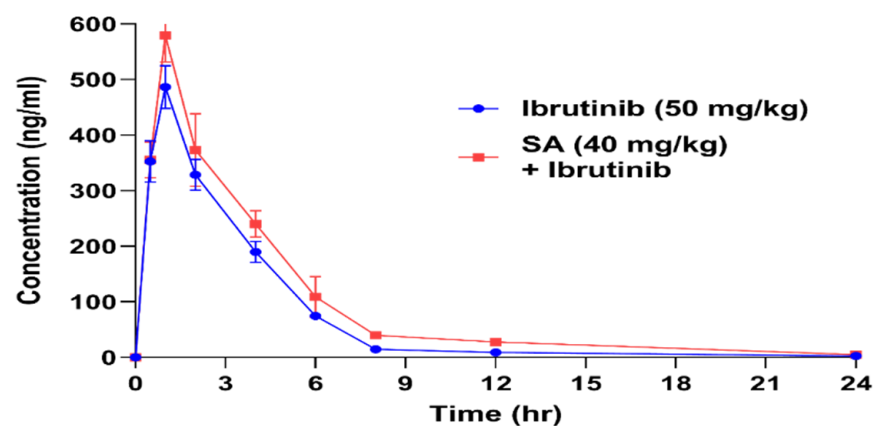


Figure 1. Plasma concentration versus time profile of IBR alone and with SA after oral administration in rats ($n = 6$).

Table 1. Non-compartmental pharmacokinetic parameters of IBR and IBR + SA following oral administration in rats.

Parameters Unit	IBR	IBR + SA	% Change Control
	Mean \pm SEM	Mean \pm SEM	
K_{el} (1/h)	0.102 \pm 0.006	0.128 \pm 0.006	24.77
$T_{1/2}$ (h)	6.92 \pm 0.42	5.50 \pm 0.26	−20.43
Cmax (ng/mL)	486.60 \pm 15.71	577.95 \pm 19.97	18.77
Clast_obs/Cmax	0.006 \pm 0.0002	0.008 \pm 0.0008	41.50
AUC _{0-t} (ng/mL h)	1694.60 \pm 50.36	2170.28 \pm 74.13	28.07
AUC _{0-inf} (ng/mL h)	1721.98 \pm 49.49	2206.71 \pm 74.087	28.15
AUC _{0-t/0-inf_obs}	0.98 \pm 0.001	0.983 \pm 0.002	−0.05
AUMC _{0-inf_obs} (ng/mL h ²)	6385.40 \pm 99.62	9624.58 \pm 648.71	50.72
MRT (0-inf_obs) h	3.72 \pm 0.07	4.34 \pm 0.211	16.87
Vz/F (mg/kg)/(ng/mL)	0.29 \pm 0.024	0.18 \pm 0.015	−37.67
Cl/F (mg/kg)/(ng/mL)/h	0.03 \pm 0.0008	0.023 \pm 0.0008	−21.82

3.2. Effect of SA on Hepatic and Intestinal CYP3A2 Protein Expression

As shown in Figure 2, the hepatic and intestinal CYP3A2 expression ($p < 0.05$) of proteins was augmented significantly by 581.30% and 231.08%, respectively, in IBR-administered rats in comparison to normal rats. Pretreatment of chronic administration of SA 40 mg/kg b.w. for 7 days to IBR-administered rats significantly inhibited hepatic and intestinal CYP3A2 protein expression by 34.30% and 35.08%, respectively, compared to IBR-administered rats. The SA 40 mg/kg pretreatment led to an inhibition of hepatic and intestinal CYP3A2 protein expression of 33.97% and 40.81% in comparison to normal rats.

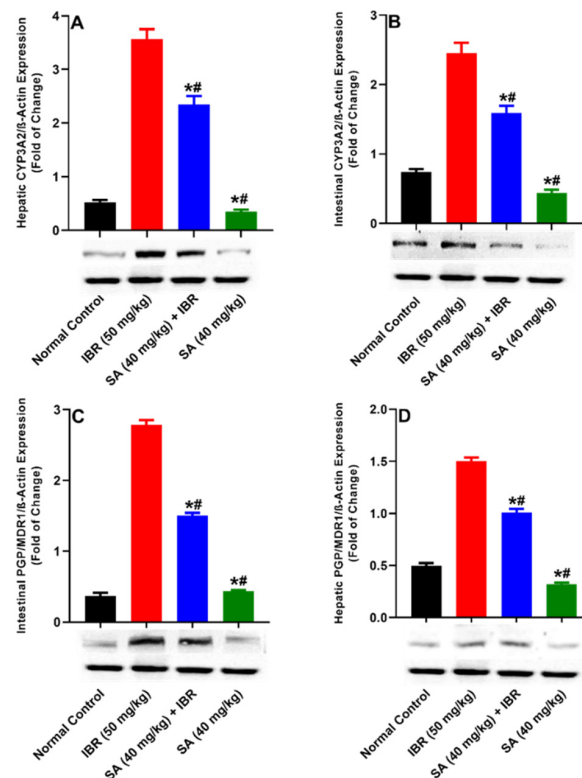


Figure 2. Hepatic CYP3A2 (A) and Pgp glycoprotein/MDR1 (D) and intestinal CYP3A2 (B) and Pgp glycoprotein/MDR1 (C) protein expression in rats after IBR administration with or without sinapic acid (SA) pretreatment. All results are presented as the average \pm SEM. * $p < 0.05$ (control); # $p < 0.05$ (IBR).

3.3. Effect of SA on Intestinal Pgp/MDR1 Protein Expression

SA was found to have an inhibitory effect on Pgp/MDR1 protein expression (Figure 2). As compared to normal control animals, PGP/MDR1 protein expression was considerably reduced in the intestine and liver of rats pretreated with SA and significantly ($p < 0.05$) increased in the intestines and livers of IBR-treated rats (661.79% and 202.88%, respectively). As compared to IBR alone, the SA-pretreated rats demonstrated a considerable suppression of IBR-induced PGP/MDR1 protein (46.11% and 32.82%, respectively). Pretreatment with SA (40 mg/kg) alone reduced hepatic and intestinal CYP3A2 protein expression by 18.58% and 35.48%, respectively, compared to controls.

4. Discussion

The usage of herbal supplements has grown substantially across the world [32,33]. The FDA does not regulate these products as rigorously as it does regular drugs [34,35]. Concomitant use of herbal medications along with conventional medicines may mimic, increase, or reduce the therapeutic effect of medicines [36]. A wide number of herbal treatments and medicines have been shown to interact with IBR. Besides its restricted therapeutic window and role as a sensitive substrate for CYP3A and Pgp/MDR1 [24,27,37], it is critical to maintaining drug concentrations to avoid side effects [37,38]. Patients are frequently unaware of potential drug–herb interactions, and some dismiss herbal supplements as medications. Significantly, clinicians are un-informed about simultaneous administration of herbal supplements that may result in plausible toxicities such as fungal infections, bleeding, sudden cardiac death, unexpected exacerbation of IBR-induced haemolytic anaemia, and severe hepatotoxicity [39,40]. Hepatoprotective, cardioprotective, and anxiolytic food supplements containing SA should be prescribed to chronic lymphocytic leukaemia (CLL) patients who require long-term treatment or consume it themselves. Several herbs have been used in traditional herbal medicines as antioxidants, hepatoprotectives, cardioprotectives, and anxiolytics, such as *Brassica chinensis*, *Brassica juncea*, *Brassica oleracea*, *Brassica nigra*, *Anacyclus pyrethrum*, *Viscum album*, *Ipomoea reniformis*, and *Zea mays* [41–46]. SA is present in plants from the Brassicaceae family and is also found in fruits (citrus and berries), tea, coffee, nuts, grains, and vegetables, among other things, and it is an integral part of human food [12,13,17].

SA is beneficial regarding oxidative stress [11], hepatoprotective [47,48], cardioprotective [49–52], gastroprotective [53], nephroprotective [54], inflammation [55], hyperglycaemia [56], neurodegeneration [55], and anxiety [57,58]. SA is widely consumed as a dietary supplement due to its chemopreventive potential. The chemopreventive oral dose of SA is 40 mg/kg b.w [25,48,51–54,59]. This is the first report on the IBR pharmacokinetic interaction with dietary supplementation of SA 40 mg/kg in rats. IBR is absorbed following oral administration and takes 1 to 2 h to reach the maximum plasma concentration (T_{max}) [10]. IBR exposure increases in patients consuming 420 mg daily; the area under the curve (AUC) was 680.52 ng h/mL [60,61]. Oral administration of IBR is rapidly absorbed in the intestine, with C_{max} , T_{max} , and AUC values of 35 ng/mL, 1–2 h, and 953 mg h/mL, respectively [24]. IBR binds to plasma proteins similarly to all other kinase inhibitors. In vitro, IBR plasma protein binding is 97.30 percent reversible, without concentration dependence (50 to 1000 ng/mL; at a steady state, the volume of the distribution ($V_d, ss/F$) was around 10,000 L) [62].

In the liver, IBR is broken down into different metabolites, predominantly by cytochrome P450 CYP3A4 [63]. The rate of biotransformation of IBR varies markedly from that of humans, with the rate elimination being several-fold faster in rats [64]. The enzymes CYP3A4 and CYP2D affect many oral drugs, including IBR. They are accountable for first-pass metabolism and alterations in absorption, drug distribution, and metabolism [5]. As a result, rats were used in the current investigation for 24-h tests. The pharmacokinetic behaviour after oral administration of IBR with or without co-administration of SA was examined using a LC/MS method [29]. Pharmacokinetic constants were obtained using the non-compartmental model. IBR was readily absorbed from the duodenum and small

intestinal epithelium into the plasma after oral administration, reaching its highest concentration (577.95 ng/mL) at 1 h post dose. The co-administration of IBR with SA displayed significant increases in C_{max} ~18.77%, $AUC_{(0-T)}$ ~28.07%, MRT ~16.87%, and K_{el} ~24.76% and a significant decrease in the volume of distribution V_z/F ~37.66%, the rate of clearance Cl/F ~21.81%, and $T_{1/2}$ ~20.43%, respectively, compared to IBR alone. This may result in increased bioavailability of IBR due to the significant inhibition of CYP3A2-facilitated metabolism of IBR in the hepatic and intestine and the inhibition of intestinal and liver Pgp/MDR1. Thus, the IBR absorption rate may increase in the intestine. These results of the pharmacokinetic parameter of IBR are consistent with previous reports exhibiting an interaction with moderate/strong CYP3A inhibitors, such as naringenin and resveratrol, which have the capacity to increase the pharmacokinetic parameters C_{max} , $AUC_{(0-T)}$, MRT, and K_{el} and decrease the V_z/F , the rate of clearance Cl/F , and $T_{1/2}$, resulting in an increase in the bioavailability of IBR [24,26,27]. The increased bioavailability may be due to inhibition of CYP3A and PGP/MDR1 in the liver and intestine, which decreases the rate of metabolism and enhances the rate of absorption in the intestine, supporting the results of previous protein expression studies. IBR induced protein expression of CYP3A and PGP/MDR1 in hepatic and intestinal tissue. Previous reports corroborate our findings, where herbal supplementation with resveratrol and naringenin altered pharmacokinetic parameters such as C_{max} and AUC of IBR due to the inhibition of CYP3A4 [26,65].

Dietary supplementation of polyphenols, such as thymoquinone, resveratrol, naringenin, apigenin, and quercetin, occurs as they are known CYP3A4 inhibitors [66–70]. SA, a polyphenol used as a supplement, has a wide range of therapeutic potential. SA exhibits *in vivo* CYP3A4/CYP2C11/PGP; inhibition at a dose of 40 mg/kg resulted in an increase in the bioavailability of carbamazepine and aripiprazole as evident by an increase in C_{max} and the AUC of these drugs [25,59]. The P-glycoprotein pump, which is situated in the brush border of the intestinal lining and is known to be inhibited by polyphenols, transports several CYP3A4, CYP2D6, and CYP2C9 substrates [71,72]. To explain the possible mechanism that increased the bioavailability of IBR, we performed Western blotting, which showed significant hepatic and intestinal CYP3A2 and PGP-MDR1 inhibition of protein expression in SA-pretreated rats. SA has the ability to modulate CYP3A/PGP-MDR1 in the liver and intestine. The protein expression data revealed that IBR significantly induced CYP A and PGP-MDR1 expression in the liver and intestine. IBR is a known CYP3A and PGP-MDR1 substrate [37]. However, increased protein expression levels of CYP3A2 and PGP-MDR1 were observed in IBR-administered rats in hepatic and intestinal proteins. The SA pretreatment significantly reduced the upregulated CYP3A2 and PGP-MDR1 protein expression in the liver and intestine of co-administered (IBR and SA) and SA-administered rats compared to the normal control. This examination proves that SA changed the pharmacokinetics of IBR via upregulation of C_{max} , AUC_{0-t} , and $T_{1/2}$, and downregulation of CL. These data are consistent with previous pharmacokinetic studies, which observed increased IBR bioavailability due to inhibition of CYP3A and PGP [24,63,73–76]. The increase in the rate of absorption of IBR in the intestine in IBR and SA co-administered rats was caused by an inhibition of P-gp/MDR1 expression [75]. However, the intensity of the rate (C_{max}) and extent (AUC) of absorption is not proportional to the intensity of the inhibition of CYP3A protein expression by SA in the IBR with SA group. These results might be due to autoinduction of CYP3A2 and PGP-MDR1 expression, which may restrict the intestinal bioavailability. Moreover, IBR is a BCS class II drug, which means it has low solubility and due to its high permeability, the absorption of IBR was rapid despite CYP3A2 inhibition in the intestine after direct intragastric administration in rats.

5. Conclusions

In brief, the co-administration of IBR with SA displayed significant increases in C_{max} , $AUC_{(0-T)}$, MRT, and K_{el} and significant decrease in the volume of distribution V_z/F , rate of clearance Cl/F , and $T_{1/2}$, respectively, compared to IBR alone. This resulted in increased bioavailability of IBR due to the significant inhibition of CYP3A2-facilitated metabolism

of IBR in the hepatic and intestine and the inhibition of intestinal and liver Pgp/MDR1. This may be due to autoinduction of CYP 3A2 and PGP-MDR1 expression, which may limit intestinal bioavailability. Moreover, despite CYP3A2 suppression in the intestine, IBR absorption was rapid after direct oral gavage in rats. This investigation clearly demonstrates that there is the potential for drug–herb interactions between SA and ibrutinib to occur, and coadministration of ibrutinib with SA or SA-containing herbs/foods should be circumvented in the clinic. Further clinical studies are required.

Limitations of the Study

The current study proposed that SA may interact with the pharmacokinetics of CYP3A/PGP substrate drugs in humans. However, since the biotransformation rate of IBR in rats differs from that in humans [77], it is difficult to quantitatively extrapolate the present results to humans. In addition, the relative role of hepatic and enteric extraction of CYP3A substrates in rats differs from that in humans; thus, the interactions with CYP3A inhibitors in rats will be different [78]. Therefore, further clinical investigations in humans are necessary to warrant such findings.

Author Contributions: Conceptualization, M.R.; Data curation, M.A.A. and A.A. (Abdul Ahad); Formal analysis, M.I., M.R., A.A. (Ajaz Ahmad), E.A.A., M.S. and A.A. (Abdul Ahad); Investigation, M.I., M.R., M.A.A., M.S. and A.A. (Abdul Ahad); Methodology, A.A. (Ajaz Ahmad), M.A.A. and M.S.; Project administration, M.R. and Y.A.B.J.; Resources, M.R. and Y.A.B.J.; Software, A.A. (Ajaz Ahmad) and M.S.; Supervision, M.R.; Validation, M.I. and E.A.A.; Visualization, Y.A.B.J., K.M.A. and F.I.A.-J.; Writing—original draft, M.R.; Writing—review and editing, M.I., M.R., A.A. (Ajaz Ahmad), K.M.A. and F.I.A.-J. All authors have read and agreed to the published version of the manuscript.

Funding: Researchers Supporting Project Number-RSP-2021/45, King Saud University.

Institutional Review Board Statement: The research was approved by the Research Ethics Committee of King Saud University College of Pharmacy Riyadh, Saudi Arabia (KSU-SE-21-58).

Data Availability Statement: All the data generated from the study is clearly presented in the manuscript.

Acknowledgments: The authors would like to extend their sincere appreciation to the Researchers Supporting Project Number-RSP-2021/45, King Saud University, Riyadh, Saudi Arabia.

Conflicts of Interest: The authors declare no conflict of interest.

References

1. Bose, P.; Gandhi, V.V.; Keating, M.J. Pharmacokinetic and pharmacodynamic evaluation of ibrutinib for the treatment of chronic lymphocytic leukemia: Rationale for lower doses. *Expert Opin. Drug Metab. Toxicol.* **2016**, *12*, 1381–1392. [[CrossRef](#)]
2. Woyach, J.A.; Johnson, A.J.; Byrd, J.C. The B-cell receptor signaling pathway as a therapeutic target in CLL. *Blood* **2012**, *120*, 1175–1184. [[CrossRef](#)]
3. Akinleye, A.; Chen, Y.; Mukhi, N.; Song, Y.; Liu, D. Ibrutinib and novel BTK inhibitors in clinical development. *J. Hematol. Oncol.* **2013**, *6*, 59. [[CrossRef](#)] [[PubMed](#)]
4. Mohamed, A.J.; Yu, L.; Backesjo, C.M.; Vargas, L.; Faryal, R.; Aints, A.; Christensson, B.; Berglof, A.; Vihinen, M.; Nore, B.F.; et al. Bruton's tyrosine kinase (Btk): Function, regulation, and transformation with special emphasis on the PH domain. *Immunol. Rev.* **2009**, *228*, 58–73. [[CrossRef](#)] [[PubMed](#)]
5. Scheers, E.; Leclercq, L.; de Jong, J.; Bode, N.; Bockx, M.; Laenen, A.; Cuyckens, F.; Skee, D.; Murphy, J.; Sukbuntherng, J.; et al. Absorption, metabolism, and excretion of oral (1)(4)C radiolabeled ibrutinib: An open-label, phase I, single-dose study in healthy men. *Drug Metab. Dispos.* **2015**, *43*, 289–297. [[CrossRef](#)] [[PubMed](#)]
6. Parmar, S.; Patel, K.; Pinilla-Ibarz, J. Ibrutinib (imbruvica): A novel targeted therapy for chronic lymphocytic leukemia. *Pharm. Ther.* **2014**, *39*, 483–519.
7. de Vries, R.; Huang, M.; Bode, N.; Jejurkar, P.; Jong, J.; Sukbuntherng, J.; Sips, L.; Weng, N.; Timmerman, P.; Verhaeghe, T. Bioanalysis of ibrutinib and its active metabolite in human plasma: Selectivity issue, impact assessment and resolution. *Bioanalysis* **2015**, *7*, 2713–2724. [[CrossRef](#)]
8. Li, G.; Huang, K.; Nikolic, D.; van Breemen, R.B. High-Throughput Cytochrome P450 Cocktail Inhibition Assay for Assessing Drug-Drug and Drug-Botanical Interactions. *Drug Metab. Dispos.* **2015**, *43*, 1670–1678. [[CrossRef](#)] [[PubMed](#)]
9. Chatterjee, P.; Franklin, M.R. Human cytochrome p450 inhibition and metabolic-intermediate complex formation by goldenseal extract and its methylenedioxyphenyl components. *Drug Metab. Dispos.* **2003**, *31*, 1391–1397. [[CrossRef](#)]

10. Advani, R.H.; Buggy, J.J.; Sharman, J.P.; Smith, S.M.; Boyd, T.E.; Grant, B.; Kolibaba, K.S.; Furman, R.R.; Rodriguez, S.; Chang, B.Y.; et al. Bruton tyrosine kinase inhibitor ibrutinib (PCI-32765) has significant activity in patients with relapsed/refractory B-cell malignancies. *J. Clin. Oncol.* **2013**, *31*, 88–94. [[CrossRef](#)]
11. Chen, C. Sinapic Acid and Its Derivatives as Medicine in Oxidative Stress-Induced Diseases and Aging. *J. Oxid. Med. Cell. Longev.* **2016**, *2016*, 3571614. [[CrossRef](#)] [[PubMed](#)]
12. Mattila, P.; Hellström, J.; Törrönen, R. Phenolic acids in berries, fruits, and beverages. *J. Agric. Food Chem.* **2006**, *54*, 7193–7199. [[CrossRef](#)] [[PubMed](#)]
13. Grosso, G.; Estruch, R.J.M. Nut consumption and age-related disease. *Maturitas* **2016**, *84*, 11–16. [[CrossRef](#)] [[PubMed](#)]
14. Van Hung, P. Phenolic compounds of cereals and their antioxidant capacity. *Crit. Rev. Food Sci. Nutr.* **2016**, *56*, 25–35. [[CrossRef](#)] [[PubMed](#)]
15. Tzagoloff, A. Metabolism of Sinapine in Mustard Plants. I. Degradation of Sinapine into Sinapic Acid & Choline. *Plant Physiol.* **1963**, *38*, 202–206. [[CrossRef](#)]
16. Chapple, C.C.; Vogt, T.; Ellis, B.E.; Somerville, C.R. An Arabidopsis mutant defective in the general phenylpropanoid pathway. *Plant Cell* **1992**, *4*, 1413–1424. [[CrossRef](#)]
17. Crozier, A.; Jaganath, I.B.; Clifford, M.N. Dietary phenolics: Chemistry, bioavailability and effects on health. *Nat. Prod. Rep.* **2009**, *26*, 1001–1043. [[CrossRef](#)]
18. Kikuzaki, H.; Hisamoto, M.; Hirose, K.; Akiyama, K.; Taniguchi, H. Antioxidant properties of ferulic acid and its related compounds. *J. Agric. Food Chem.* **2002**, *50*, 2161–2168. [[CrossRef](#)]
19. Zou, Y.-N.; Kim, A.-R.; Kim, J.-E.; Park, T.-H.; Choi, J.-S.; Chung, H.-Y. Peroxynitrite scavenging activity of sinapic acid (3, 5-dimethoxy-4-hydroxycinnamic acid) isolated from Brassica juncea. *J. Agric. Food Chem.* **2002**, *50*, 5884–5890. [[CrossRef](#)]
20. Szwajgier, D.; Borowiec, K.; Pustelniak, K. The neuroprotective effects of phenolic acids: Molecular mechanism of action. *Nutrients* **2017**, *9*, 477. [[CrossRef](#)]
21. Ziauddeen, N.; Rosi, A.; Del Rio, D.; Amoutzopoulos, B.; Nicholson, S.; Page, P.; Scazzina, F.; Brighenti, F.; Ray, S.; Mena, P. Dietary intake of (poly)phenols in children and adults: Cross-sectional analysis of UK National Diet and Nutrition Survey Rolling Programme (2008–2014). *Eur. J. Nutr.* **2019**, *58*, 3183–3198. [[CrossRef](#)] [[PubMed](#)]
22. Radtke, J.; Linseisen, J.; Wolfram, G. Phenolic acid intake of adults in a Bavarian subgroup of the national food consumption survey. *Z. Ernähr.* **1998**, *37*, 190–197. [[CrossRef](#)]
23. Zuo, Y.; Wang, C.; Zhan, J. Separation, characterization, and quantitation of benzoic and phenolic antioxidants in American cranberry fruit by GC-MS. *J. Agric. Food Chem.* **2002**, *50*, 3789–3794. [[CrossRef](#)] [[PubMed](#)]
24. de Zwart, L.; Snoeys, J.; De Jong, J.; Sukbuntherng, J.; Mannaert, E.; Monshouwer, M. Ibrutinib Dosing Strategies Based on Interaction Potential of CYP3A4 Perpetrators Using Physiologically Based Pharmacokinetic Modeling. *Clin. Pharmacol. Ther.* **2016**, *100*, 548–557. [[CrossRef](#)] [[PubMed](#)]
25. Raish, M.; Ahmad, A.; Ansari, M.A.; Alkharfy, K.M.; Ahad, A.; Khan, A.; Aljenobi, F.I.; Ali, N.; Al-Mohizea, A.M. Effect of sinapic acid on aripiprazole pharmacokinetics in rats: Possible food drug interaction. *J. Food Drug Anal.* **2019**, *27*, 332–338. [[CrossRef](#)]
26. Wen, J.; Bao, S.S.; Zhang, B.W.; Liu, T.H.; Ou-Yang, Q.G.; Cai, J.P.; Zhou, H.Y. Inhibitory effect of resveratrol on the pharmacokinetic of ibrutinib by UPLC-MS/MS. *Drug Dev. Ind. Pharm.* **2019**, *45*, 27–31. [[CrossRef](#)]
27. Liu, J.; Liu, H.; Zeng, Q. The effect of naringenin on the pharmacokinetics of ibrutinib in rat: A drug-drug interaction study. *Biomed. Chromatogr.* **2019**, *33*, e4507. [[CrossRef](#)]
28. de Vries, R.; Smit, J.W.; Helleman, P.; Jiao, J.; Murphy, J.; Skee, D.; Snoeys, J.; Sukbuntherng, J.; Vliegen, M.; de Zwart, L.; et al. Stable isotope-labelled intravenous microdose for absolute bioavailability and effect of grapefruit juice on ibrutinib in healthy adults. *Br. J. Clin. Pharmacol.* **2016**, *81*, 235–245. [[CrossRef](#)]
29. Iqbal, M.; Shakeel, F.; Anwer, T. Simple and Sensitive UPLC-MS/MS Method for High-Throughput Analysis of Ibrutinib in Rat Plasma: Optimization by Box-Behnken Experimental Design. *J. AOAC Int.* **2016**, *1*, 618–625. [[CrossRef](#)]
30. Smith, P.K.; Krohn, R.I.; Hermanson, G.T.; Mallia, A.K.; Gartner, F.H.; Provenzano, M.D.; Fujimoto, E.K.; Goeke, N.M.; Olson, B.J.; Klenk, D.C. Measurement of protein using bicinchoninic acid. *Anal. Biochem.* **1985**, *150*, 76–85. [[CrossRef](#)]
31. Towbin, H.; Staehelin, T.; Gordon, J. Electrophoretic transfer of proteins from polyacrylamide gels to nitrocellulose sheets: Procedure and some applications. *Proc. Natl. Acad. Sci. USA* **1979**, *76*, 4350–4354. [[CrossRef](#)] [[PubMed](#)]
32. Ekor, M. The growing use of herbal medicines: Issues relating to adverse reactions and challenges in monitoring safety. *Front. Pharmacol.* **2014**, *4*, 177. [[CrossRef](#)]
33. Kelly, J.P.; Kaufman, D.W.; Kelley, K.; Rosenberg, L.; Anderson, T.E.; Mitchell, A.A. Recent trends in use of herbal and other natural products. *Arch. Intern. Med.* **2005**, *165*, 281–286. [[CrossRef](#)] [[PubMed](#)]
34. Bauer, B.A. Herbal therapy: What a clinician needs to know to counsel patients effectively. *Mayo Clin. Proc.* **2000**, *75*, 835–841. [[CrossRef](#)]
35. Miller, L.G.; Hume, A.; Harris, I.M.; Jackson, E.A.; Kanmaz, T.J.; Cauffield, J.S.; Chin, T.W.; Knell, M. White paper on herbal products. American College of Clinical Pharmacy. *Pharmacotherapy* **2000**, *20*, 877–891. [[CrossRef](#)] [[PubMed](#)]
36. Fugh-Berman, A.; Ernst, E. Herb-drug interactions: Review and assessment of report reliability. *Br. J. Clin. Pharmacol.* **2001**, *52*, 587–595. [[CrossRef](#)] [[PubMed](#)]

37. Tapaninen, T.; Olkkola, A.M.; Tornio, A.; Neuvonen, M.; Elonen, E.; Neuvonen, P.J.; Niemi, M.; Backman, J.T. Itraconazole Increases Ibrutinib Exposure 10-Fold and Reduces Interindividual Variation—A Potentially Beneficial Drug-Drug Interaction. *Clin. Transl. Sci.* **2020**, *13*, 345–351. [[CrossRef](#)] [[PubMed](#)]
38. Lambert Kuhn, E.; Leveque, D.; Lioure, B.; Gourieux, B.; Bilbault, P. Adverse event potentially due to an interaction between ibrutinib and verapamil: A case report. *J. Clin. Pharm. Ther.* **2016**, *41*, 104–105. [[CrossRef](#)]
39. Tafesh, Z.H.; Coleman, M.; Fulmer, C.; Nagler, J. Severe Hepatotoxicity due to Ibrutinib with a Review of Published Cases. *Case Rep. Gastroenterol.* **2019**, *13*, 357–363. [[CrossRef](#)]
40. Levy, I.; Polliack, A.; Tadmor, T. Five Ibrutinib-Associated Side Effects That All Clinicians Should Be Aware of. *Acta Haematol.* **2019**, *141*, 254–255. [[CrossRef](#)]
41. Ray, L.R.; Alam, M.S.; Junaid, M.; Ferdousy, S.; Akter, R.; Hosen, S.M.Z.; Mouri, N.J. Brassica oleracea var. capitata f. alba: A review on its botany, traditional uses, phytochemistry and pharmacological activities. *Mini Rev. Med. Chem.* **2021**, *21*, 2399–2417. [[CrossRef](#)]
42. Favela-Gonzalez, K.M.; Hernandez-Almanza, A.Y.; De la Fuente-Salcido, N.M. The value of bioactive compounds of cruciferous vegetables (Brassica) as antimicrobials and antioxidants: A review. *J. Food Biochem.* **2020**, *44*, e13414. [[CrossRef](#)] [[PubMed](#)]
43. Morales-Lopez, J.; Centeno-Alvarez, M.; Nieto-Camacho, A.; Lopez, M.G.; Perez-Hernandez, E.; Perez-Hernandez, N.; Fernandez-Martinez, E. Evaluation of antioxidant and hepatoprotective effects of white cabbage essential oil. *Pharm. Biol.* **2017**, *55*, 233–241. [[CrossRef](#)]
44. Gupta, G.; Kazmi, I.; Afzal, M.; Rahman, M.; Saleem, S.; Ashraf, M.S.; Khusroo, M.J.; Nazeer, K.; Ahmed, S.; Mujeeb, M.; et al. Sedative, antiepileptic and antipsychotic effects of *Viscum album* L. (Loranthaceae) in mice and rats. *J. Ethnopharmacol.* **2012**, *141*, 810–816. [[CrossRef](#)] [[PubMed](#)]
45. Sankhari, J.M.; Thounaojam, M.C.; Jadeja, R.N.; Devkar, R.V.; Ramachandran, A.V. Anthocyanin-rich red cabbage (*Brassica oleracea* L.) extract attenuates cardiac and hepatic oxidative stress in rats fed an atherogenic diet. *J. Sci. Food Agric.* **2012**, *92*, 1688–1693. [[CrossRef](#)] [[PubMed](#)]
46. Mukherjee, S.; Lekli, I.; Ray, D.; Gangopadhyay, H.; Raychaudhuri, U.; Das, D.K. Comparison of the protective effects of steamed and cooked broccolis on ischaemia-reperfusion-induced cardiac injury. *Br. J. Nutr.* **2010**, *103*, 815–823. [[CrossRef](#)] [[PubMed](#)]
47. Pandi, A.; Kalappan, V.M. Pharmacological and therapeutic applications of Sinapic acid—An updated review. *Mol. Biol. Rep.* **2021**, *48*, 3733–3745. [[CrossRef](#)]
48. Shin, D.S.; Kim, K.W.; Chung, H.Y.; Yoon, S.; Moon, J.O. Effect of sinapic acid against dimethylnitrosamine-induced hepatic fibrosis in rats. *Arch. Pharm. Res.* **2013**, *36*, 608–618. [[CrossRef](#)]
49. Yun, U.J.; Yang, D.K. Sinapic Acid Inhibits Cardiac Hypertrophy via Activation of Mitochondrial Sirt3/SOD2 Signaling in Neonatal Rat Cardiomyocytes. *Antioxidants* **2020**, *9*, 1163. [[CrossRef](#)]
50. Alaofi, A.L. Sinapic Acid Ameliorates the Progression of Streptozotocin (STZ)-Induced Diabetic Nephropathy in Rats via NRF2/HO-1 Mediated Pathways. *Front. Pharmacol.* **2020**, *11*, 1119. [[CrossRef](#)]
51. Stanely Mainzen Prince, P.; Dey, P.; Roy, S.J. Sinapic acid safeguards cardiac mitochondria from damage in isoproterenol-induced myocardial infarcted rats. *J. Biochem. Mol. Toxicol.* **2020**, *34*, e22556. [[CrossRef](#)] [[PubMed](#)]
52. Silambarasan, T.; Manivannan, J.; Priya, M.K.; Suganya, N.; Chatterjee, S.; Raja, B. Sinapic acid protects heart against ischemia/reperfusion injury and H9c2 cardiomyoblast cells against oxidative stress. *Biochem. Biophys. Res. Commun.* **2015**, *456*, 853–859. [[CrossRef](#)] [[PubMed](#)]
53. Ansari, M.A.; Raish, M.; Bin Jardan, Y.A.; Ahmad, A.; Shahid, M.; Ahmad, S.F.; Haq, N.; Khan, M.R.; Bakheet, S.A. Sinapic acid ameliorates D-galactosamine/lipopolysaccharide-induced fulminant hepatitis in rats: Role of nuclear factor erythroid-related factor 2/heme oxygenase-1 pathways. *World J. Gastroenterol.* **2021**, *27*, 592–608. [[CrossRef](#)] [[PubMed](#)]
54. Ansari, M.A.; Raish, M.; Ahmad, A.; Alkharfy, K.M.; Ahmad, S.F.; Attia, S.M.; Alsaad, A.M.S.; Bakheet, S.A. Sinapic acid ameliorate cadmium-induced nephrotoxicity: In vivo possible involvement of oxidative stress, apoptosis, and inflammation via NF-kappaB downregulation. *Environ. Toxicol. Pharmacol.* **2017**, *51*, 100–107. [[CrossRef](#)]
55. Verma, V.; Singh, D.; Kh, R. Sinapic Acid Alleviates Oxidative Stress and Neuro-Inflammatory Changes in Sporadic Model of Alzheimer's Disease in Rats. *Brain Sci.* **2020**, *10*, 923. [[CrossRef](#)]
56. Cherng, Y.G.; Tsai, C.C.; Chung, H.H.; Lai, Y.W.; Kuo, S.C.; Cheng, J.T. Antihyperglycemic action of sinapic acid in diabetic rats. *J. Agric. Food Chem.* **2013**, *61*, 12053–12059. [[CrossRef](#)]
57. Harsha, S.N.; Anilakumar, K.R. Anxiolytic property of *Lactuca sativa*, effect on anxiety behaviour induced by novel food and height. *Asian Pac. J. Trop. Med.* **2013**, *6*, 532–536. [[CrossRef](#)]
58. Yoon, B.H.; Jung, J.W.; Lee, J.J.; Cho, Y.W.; Jang, C.G.; Jin, C.; Oh, T.H.; Ryu, J.H. Anxiolytic-like effects of sinapic acid in mice. *Life Sci.* **2007**, *81*, 234–240. [[CrossRef](#)]
59. Raish, M.; Ahmad, A.; Ansari, M.A.; Alkharfy, K.M.; Ahad, A.; Al-Jenoobi, F.I.; Al-Mohizea, A.M.; Khan, A.; Ali, N. Effects of sinapic acid on hepatic cytochrome P450 3A2, 2C11, and intestinal P-glycoprotein on the pharmacokinetics of oral carbamazepine in rats: Potential food/herb-drug interaction. *Epilepsy Res.* **2019**, *153*, 14–18. [[CrossRef](#)]
60. Raedler, L.A. Imbruvica (Ibrutinib) First Drug Approved Specifically for Marginal-Zone Lymphoma. *Drug Updates* **2017**, *10*.
61. Raedler, L.A. Imbruvica (Ibrutinib) First Drug Approved Specifically for Marginal-Zone Lymphoma and for Chronic Graft-versus-Host Disease. *Am. Health Drug Benefits* **2018**, *11*.

62. Marostica, E.; Sukbuntherng, J.; Loury, D.; de Jong, J.; de Trixhe, X.W.; Vermeulen, A.; De Nicolao, G.; O'Brien, S.; Byrd, J.C.; Advani, R.; et al. Population pharmacokinetic model of ibrutinib, a Bruton tyrosine kinase inhibitor, in patients with B cell malignancies. *Cancer Chemother. Pharmacol.* **2015**, *75*, 111–121. [[CrossRef](#)] [[PubMed](#)]
63. de Jong, J.; Skee, D.; Murphy, J.; Sukbuntherng, J.; Hellemans, P.; Smit, J.; de Vries, R.; Jiao, J.J.; Snoeys, J.; Mannaert, E. Effect of CYP3A perpetrators on ibrutinib exposure in healthy participants. *Pharmacol. Res. Perspect.* **2015**, *3*, e00156. [[CrossRef](#)] [[PubMed](#)]
64. Fabrizi, L.; Gemma, S.; Testai, E.; Vittozzi, L. Identification of the cytochrome P450 isoenzymes involved in the metabolism of diazinon in the rat liver. *J. Biochem. Mol. Toxicol.* **1999**, *13*, 53–61. [[CrossRef](#)]
65. Wang, B.; Shen, J.; Zhou, Q.; Meng, D.; He, Y.; Chen, F.; Wang, S.; Ji, W. Effects of naringenin on the pharmacokinetics of tofacitinib in rats. *Pharm. Biol.* **2020**, *58*, 225–230. [[CrossRef](#)] [[PubMed](#)]
66. Saric Mustapic, D.; Debeljak, Z.; Males, Z.; Bojic, M. The Inhibitory Effect of Flavonoid Aglycones on the Metabolic Activity of CYP3A4 Enzyme. *Molecules* **2018**, *23*, 2553. [[CrossRef](#)]
67. Albassam, A.A.; Ahad, A.; Alsultan, A.; Al-Jenoobi, F.I. Inhibition of cytochrome P450 enzymes by thymoquinone in human liver microsomes. *Saudi Pharm. J.* **2018**, *26*, 673–677. [[CrossRef](#)] [[PubMed](#)]
68. Guthrie, A.R.; Chow, H.S.; Martinez, J.A. Effects of resveratrol on drug- and carcinogen-metabolizing enzymes, implications for cancer prevention. *Pharmacol. Res. Perspect.* **2017**, *5*, e00294. [[CrossRef](#)]
69. Ho, P.C.; Saville, D.J.; Coville, P.F.; Wanwimolruk, S. Content of CYP3A4 inhibitors, naringin, naringenin and bergapten in grapefruit and grapefruit juice products. *Pharm. Acta Helv.* **2000**, *74*, 379–385. [[CrossRef](#)]
70. Rashid, J.; McKinstry, C.; Renwick, A.G.; Dirnhuber, M.; Waller, D.G.; George, C.F. Quercetin, an in vitro inhibitor of CYP3A, does not contribute to the interaction between nifedipine and grapefruit juice. *Br. J. Clin. Pharmacol.* **1993**, *36*, 460–463. [[CrossRef](#)]
71. Kitagawa, S. Inhibitory effects of polyphenols on p-glycoprotein-mediated transport. *Biol. Pharm. Bull.* **2006**, *29*, 1–6. [[CrossRef](#)]
72. Jodoin, J.; Demeule, M.; Beliveau, R. Inhibition of the multidrug resistance P-glycoprotein activity by green tea polyphenols. *Biochim. Biophys. Acta* **2002**, *1542*, 149–159. [[CrossRef](#)]
73. Dutreix, C.; Lorenzo, S.; Wang, Y. Comparison of two endogenous biomarkers of CYP3A4 activity in a drug-drug interaction study between midostaurin and rifampicin. *Eur. J. Clin. Pharmacol.* **2014**, *70*, 915–920. [[CrossRef](#)] [[PubMed](#)]
74. Marde Arrhen, Y.; Nysten, H.; Lovgren-Sandblom, A.; Kanebratt, K.P.; Wide, K.; Diczfalusy, U. A comparison of 4beta-hydroxycholesterol: Cholesterol and 6beta-hydroxycortisol: Cortisol as markers of CYP3A4 induction. *Br. J. Clin. Pharmacol.* **2013**, *75*, 1536–1540. [[CrossRef](#)] [[PubMed](#)]
75. Van Hoppe, S.; Rood, J.J.M.; Buil, L.; Wagenaar, E.; Sparidans, R.W.; Beijnen, J.H.; Schinkel, A.H. P-Glycoprotein (MDR1/ABCB1) Restricts Brain Penetration of the Bruton's Tyrosine Kinase Inhibitor Ibrutinib, While Cytochrome P450-3A (CYP3A) Limits Its Oral Bioavailability. *Mol. Pharm.* **2018**, *15*, 5124–5134. [[CrossRef](#)] [[PubMed](#)]
76. De Jong, J.; Sukbuntherng, J.; Skee, D.; Murphy, J.; O'Brien, S.; Byrd, J.C.; James, D.; Hellemans, P.; Loury, D.J.; Jiao, J.; et al. The effect of food on the pharmacokinetics of oral ibrutinib in healthy participants and patients with chronic lymphocytic leukemia. *Cancer Chemother. Pharmacol.* **2015**, *75*, 907–916. [[CrossRef](#)]
77. Faigle, J.; Feldman, K. *Carbamazepine. Chemistry and Biotransformation, in Anti-Epileptic Drugs*, 4th ed.; Levy, R.H., Mattson, R.H., Meldrum, B.S., Eds.; Raven Press: New York, NY, USA, 1995.
78. Kotegawa, T.; Laurijssens, B.E.; Von Moltke, L.L.; Cotreau, M.M.; Perloff, M.D.; Venkatakrishnan, K.; Warrington, J.S.; Granda, B.W.; Harmatz, J.S.; Greenblatt, D.J. In vitro, pharmacokinetic, and pharmacodynamic interactions of ketoconazole and midazolam in the rat. *J. Pharmacol. Exp. Ther.* **2002**, *302*, 1228–1237. [[CrossRef](#)] [[PubMed](#)]